arXiv:1609.09483v1 [physics.ins-det] 29 Sep 2016

In-Situ Measurement of Relative Attenuation Length of Gadolinium-Loaded Liquid Scintillator Using Source Data at RENO Experiment

H. S. Kim[g,*], S. Y. Kim[h], J. H. Choi[b], W.Q. Choi[h,2], Y. Choi[j], H. I. Jang[i], J. S. Jang[c], K. K. Joo[a], B. R. Kim[a], J. Y. Kim[a], S. B. Kim[h], W. Kim[f], E. Kwon[h], D. H. Lee[h], I. T. Lim[a], M. Y. Pac[b], I. G. Park[e], J. S. Park[h,1], R. G. Park[a], H. Seo[h], S. H. Seo[h], Y. G. Seon[f], C. D. Shin[a], J. H. Yang[j], I. S. Yeo[a], I. Yu[j]

[a] *Institute for Universe and Elementary Particles, Chonnam National University, Gwangju 61186, Korea*
[b] *Department of Radiology, Dongshin University, Naju 58245, Korea*
[c] *GIST College, Gwangju Institute of Science and Technology, Gwangju 61005, Korea*
[d] *Institute for Basic Science, Daejeon 34047, Korea*
[e] *Department of Physics, Gyeongsang National University, Jinju 52828, Korea*
[f] *Department of Physics, Kyungpook National University, Daegu 41566, Korea*
[g] *Department of Physics and Astronomy, Sejong University, Seoul 05006, Korea*
[h] *Department of Physics and Astronomy, Seoul National University, Seoul 08826, Korea*
[i] *Department of Fire Safety, Seoyeong University, Gwangju 61268, Korea*
[j] *Department of Physics, Sungkyunkwan University, Suwon 16419, Korea*

Abstract

We present an *in-situ* method of measuring the relative attenuation length of gadolinium-loaded liquid scintillator in the RENO detectors using radioactive source calibration data without requiring any PMT performance model. We observed the degradation of the attenuation length of the gadolinium-loaded liquid scintillator in the RENO detectors by ∼50% over a period of about 4 years.

Keywords: RENO, Liquid scintillator, Attenuation length
PACS: 78.20.Ci, 29.40.Mc

1. Introduction

The stability of the liquid scintillator (LS) is a major concern for neutrino experiments using LS especially that last several years. Particularly important for large volume LS detectors is the stability of the attenuation length of LS as the degradation of the attenuation length would greatly affect the detector performance such as the energy measurement as well as the vertex determination. It has been reported that the gadolinium-loaded LS (Gd-LS) has shown the degradation of the attenuation length over a relatively short period of time [1, 2]. The RENO experiment also has experienced degradation of the attenuation length in its Gd-LS [3].

To correct for the effects of the deteriorating detector performance due to the degradation of the LS attenuation length, it is important to monitor the change in the attenuation length. The attenuation length of LS in the detector can be measured with LS sampled from the detector using either spectrophotometers or instruments built specifically for the purpose. Commercially available spectrophotometers use a light source with various wavelengths and measure the attenuation length of the liquid samples in small cuvettes. Because of the limitation in the sample dimension, which is typically on the order of a ten centimeters, the uncertainty on the attenuation length measurement can be large if the attenuation length is on the order of ten meters or larger. Specifically built instruments such as the one used in Ref. [4] have shown to achieve a sub-meter uncertainty for an order of a 10 m attenuation length LS. However, they require several liters of the LS to make a measurement and this limits the frequency of the measurements on the LS sampled fresh from the detector. Also the environmental conditions such as temperature which the LS sample is

*Corresponding author. Tel: +82 2 3408 3397 Fax: +82 2 3408 4316
Email address: hyunsookim@sejong.ac.kr (H. S. Kim)
[1] Present Address: Institute for Basic Science, Daejeon 34047, Korea
[2] Present Address: Korea Institute of Science and Technology Information, Daejeon 34141, Korea

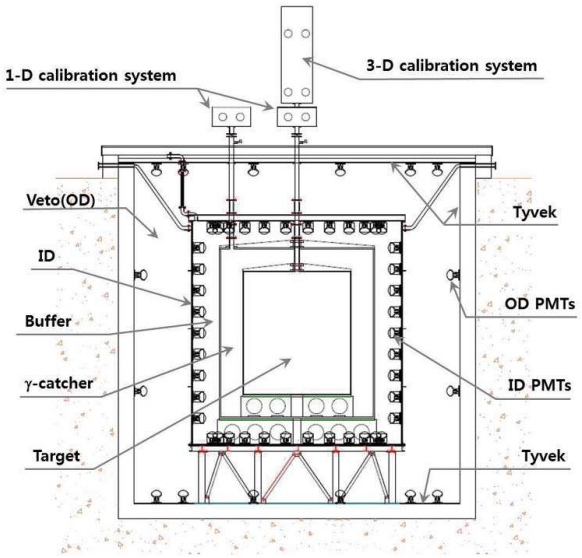

Figure 1: A cutaway view of a RENO detector. There are two 1-D calibration systems each for target and γ-catcher, that deploy radioactive sources vertically (z-direction).

handled under once taken out of the detector may differ from the conditions in the detector. This makes the prolonged measurement less reliable in such instruments as a true attenuation length of the LS in the detector.

Alternatively, the attenuation length of LS can be measured *in-situ* using radioactive sources in the detector [2]. In such a case, the attenuation length measured is for the same optical photon spectrum as the scintillation signal in the experiment. However, this method requires detailed modeling of PMT performances for each PMT used for the measurement.

In this paper we report an *in-situ* method of measuring the relative attenuation length of Gd-LS in the RENO detectors and the results of the measurements using calibration source data samples spanning about 1 300 days. This method does not require a PMT performance model.

2. RENO Detector

The RENO detector is described in details in Ref. [6] and only the relevant part will be briefly described here. Figure 1 shows a schematic view of RENO detector. There are two identical detectors, near and far detectors, for RENO experiment. Each detector consists of inner and outer detectors, where the latter is used for cosmic muon rejection. The inner detector is contained in a cylindrical stainless steel vessel with two nested concentric transparent acrylic vessels. The innermost vessel holds 16 tons of linear alkylbenzene (LAB) based Gd-LS, target, with a 0.1% Gd concentration. In between the target vessel and the outer vessel holds a 60 cm thick layer of a unloaded LS, γ-catcher, that recovers energy leakage from the target. The thicknesses of the target and γ-catcher vessel walls are 2.5 cm and 3.0 cm, respectively. A 70 cm thick buffer region filled with 65 tons of mineral oil (MO) surrounds the γ-catcher. The light signals from the inner detector are detected by 354 Hamamatsu R7081 10-inch photomultipliers (PMTs) mounted perpendicularly on the inner wall of the stainless steel vessel and immersed in the buffer. The gain of each PMT is measured before the installation and continually corrected for the gain drift. The refractive indices for Gd-LS, LS, MO, and acrylic vessels at 405 nm are measured to be 1.50, 1.50, 1.47, and 1.50, respectively [7, 8]. Therefore, no significant reflection or refraction is expected at the medium interfaces. Table 1 shows the dimensions of the detector.

There are two 1-D source calibration systems on each detector; one for deploying a source in the target and the other for the γ-catcher both in the vertical direction (z-direction). Only the calibration system for the

Layer	Outer Diameter (cm)	Outer Height (cm)	Material
Target	275.0	315.0	Gd-LS
Target Vessel	280.0	320.0	Acrylic Plastic
γ-Catcher	394.0	434.0	LS
γ-Catcher Vessel	400.0	440.0	Acrylic Plastic
Buffer	538.8	578.8	MO
Buffer Vessel	540.0	580.0	Stainless Steel
Veto	840.0	889.8	Water

Table 1: The dimensions of detector layers. The layers are in a concentric cylindrical shape.

Detector	Date	Source z-position Intervals (cm)
Far	2011-11-08 (99)	40
	2012-07-13 (347)	40
	2012-10-27 (453)	40
	2013-12-09 (861)	40
	2014-01-17 (900)	10
	2015-04-14 (1 352)	10
Near	2011-11-10 (101)	40
	2012-04-19 (262)	40
	2012-07-12 (346)	40
	2012-10-27 (453)	40
	2013-12-09 (861)	40
	2014-01-18 (901)	10
	2015-04-13 (1 351)	10

Table 2: List of ^{60}Co source calibration data used in the relative attenuation length of the target Gd-LS measurement. The source is positioned between $z = \pm 120$ cm. The numbers within the parentheses are the elapsed time in days since 2011-08-01, which is approximately when the RENO detectors became operational.

target is used for this measurement where the source moves along the axial centerline of the target in the z-direction. A radioactive source housed in a Teflon-PFA container is attached at the end of a polyethylene wire that is driven by a stepper motor. A weight is attached to the source container to counteract the buoyant force when the source is submerged in the liquid. The relative z-position accuracy of the source is measured to be an order of a few millimeters and the systematic uncertainty in the shift in the z-position is expected to be a few centimeters.

3. Data and Event Selection

For this study the calibration data using a ^{60}Co radioactive source taken between Nov. 2011 and April 2015 are used. The source is positioned between $z = -120$ and 120 cm in the target, where $(x, y, z) = (0, 0, 0)$ is the center of the target. Table 2 shows the dates of the data samples taken for this measurement.
The event vertex was reconstructed for each event using the weighting method described in Ref. [9]. Figure 2 shows the reconstructed event vertex distributions of a calibration data sample for the far detector. The event vertex distributions in x-y, y-z, and z-x are fit with 2-D Gaussian functions simultaneously. For each event the vertex position (x, y, z) is measured and the events satisfying the following condition are used:

$$\frac{(x-\bar{x})^2}{\sigma_x^2} + \frac{(y-\bar{y})^2}{\sigma_y^2} + \frac{(z-\bar{z})^2}{\sigma_z^2} < 1. \quad (1)$$

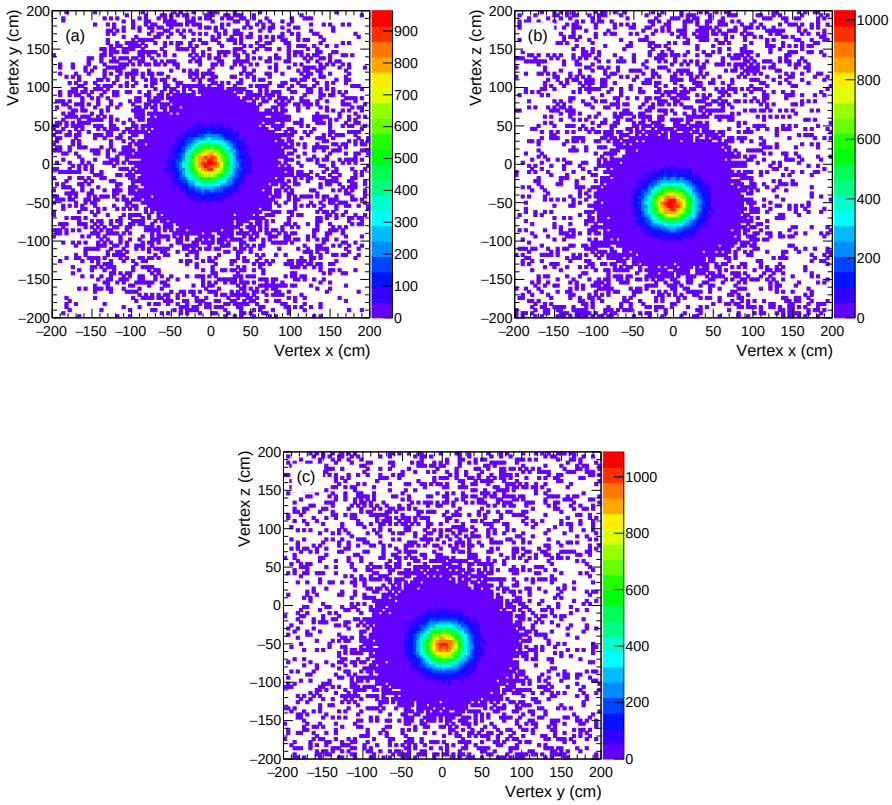

Figure 2: The reconstructed event vertex distributions in (a) x-y, (b) x-z, and (c) y-z of the data taken at 2014-01-17 at far detector. A ^{60}Co source is located at nominal $z = -50$ cm. The widths of the distributions are ~ 20 cm in all directions.

Here $(\bar{x}, \bar{y}, \bar{z})$ and $(\sigma_x, \sigma_y, \sigma_z)$ are the means and widths, respectively, of the 2-D Gaussian from the best fits. This event vertex requirement ensures that the event occurred at the desired vertex position and removes most of background events. No other event selection requirement is used.

4. Method of Relative Attenuation Length Measurement

When a radioactive source is submerged in a liquid scintillator, particles from the source lose their energy in the immediate vicinity of the source and optical photons from the scintillating process are radiated isotropically. In a uniform medium, if a light source emits N optical photons isotropically at $\vec{r}$ from a PMT pointing in the unit vector $\hat{\xi}$ direction, then the number of photons detected by the PMT, n, can be written as

$$n = N \frac{\Omega(\vec{r}, \hat{\xi})}{4\pi} \epsilon(\vec{r}, \hat{\xi}) \exp(-r/\lambda), \tag{2}$$

where $\Omega(\vec{r}, \hat{\xi})$ is the PMT coverage in solid angle, $\epsilon(\vec{r}, \hat{\xi})$ is the PMT efficiency, and λ is the attenuation length of the medium.

A light must traverse three layers of liquids in target (t), γ-catcher (c), and buffer (b), and two layers of acrylic vessel walls to reach any PMT in the inner detector from anywhere in the target of the RENO

detector. Then the ratio of numbers of photons detected by any two PMTs i and j is

$$\begin{aligned}\frac{n_i}{n_j} &= \frac{\Omega_i\,\epsilon_i\prod_\ell \exp(-r_i^{(\ell)}/\lambda^{(\ell)})}{\Omega_j\,\epsilon_j\prod_\ell \exp(-r_j^{(\ell)}/\lambda^{(\ell)})} \\ &= \frac{\Omega_i\,\epsilon_i}{\Omega_j\,\epsilon_j}\exp\left(-\sum_\ell \frac{\Delta r_{ij}^{(\ell)}}{\lambda^{(\ell)}}\right), \end{aligned} \tag{3}$$

where $\Delta r_{ij}^{(\ell)} \equiv r_i^{(\ell)} - r_j^{(\ell)}$ in layer ℓ, $\Omega_i \equiv \Omega(\vec{r}_i, \hat{\xi}_i)$, and $\epsilon_i \equiv \epsilon(\vec{r}_i, \hat{\xi}_i)$. Here $\hat{\xi}_i$ is the unit vector in the direction that the i^{th} PMT is pointing. If $|\Delta r^{(\ell)}/\lambda^{(\ell)}|$ ($\ell \neq t$) can be made much smaller than $|\Delta r^{(t)}/\lambda^{(t)}|$ then Eq. 3 can be approximated as a function of parameters involving only the target as

$$\frac{n_i}{n_j} \simeq \frac{\Omega_i\epsilon_i}{\Omega_j\epsilon_j}\exp\left(-\frac{\Delta r_{ij}^{(t)}}{\lambda^{(t)}}\right). \tag{4}$$

A similar technique has been used to measure the attenuation length of Gd-LS in at CHOOZ experiment [2] where the CHOOZ detector has only the target to consider. For the RENO detectors this condition can be satisfied using sets of six PMTs each installed at top and bottom closest to the axial centerline of the target, which the target calibration sources are deployed along. The schematics of the arrangement of these PMTs relevant to this study is shown in Fig. 3. For the source positions at $z = \pm 120$ cm, where the effects from the other layers are the greatest in the data used in this study, the deviations in n_i/n_j coming from the other layers are estimated to be less than 1%. The effects of the uniform changes in attenuation lengths in non-target layers over time to the measurement should be negligible as well. Since these six PMTs in each set have the same distance and polar angle from the source, they are treated as a single PMT. Henceforth, the top six PMTs shall be labeled as "u" and the bottom six shall be labeled as "d."

Using the six equidistance PMTs from the detector centerline on each side also reduces uncertainties coming from the hit position dependent efficiency variation on the PMT cathode by averaging out on six PMTs. However, despite using these PMTs it is found that the measurement based on Eq. 4 is very sensitive to the modeling of the PMT performance, thereby making the measurement of the attenuation length very dependent on the model.

Although it may not be feasible to measure the attenuation length using Eq. 4, due to lack of an accurate PMT's performance model, it is possible to extract the relative attenuation length with respect to the reference attenuation length at a given time. Rewriting Eq. 4 as a function of time and defining it as $R_{ud}(t)$ give [3]

$$\begin{aligned} R_{ud}(t) &\equiv \frac{n_u(t)}{n_d(t)} \\ &= \frac{\Omega_u\epsilon_u(t)}{\Omega_d\epsilon_d(t)}\exp\left(-\frac{\Delta r_{ud}}{\lambda(t)}\right), \end{aligned} \tag{5}$$

where $\epsilon_{u(d)}(t) = \epsilon(\vec{r}_{u(d)}, \hat{\xi}_{u(d)}, t)$. Taking the ratio of $R_{ud}(t)$'s obtained at two different times t_1 and t_2 gives

$$\begin{aligned}\frac{R_{ud}(t_1)}{R_{ud}(t_2)} &= \frac{\frac{\Omega_u\epsilon_u(t_1)}{\Omega_d\epsilon_d(t_1)}\exp\left(-\Delta r_{ud}/\lambda(t_1)\right)}{\frac{\Omega_u\epsilon_u(t_2)}{\Omega_d\epsilon_d(t_2)}\exp\left(-\Delta r_{ud}/\lambda(t_2)\right)} \\ &= \frac{\epsilon_u(t_1)\epsilon_d(t_2)}{\epsilon_u(t_2)\epsilon_d(t_1)}\exp\left(-\frac{\Delta r_{ud}}{\lambda_m(t_1,t_2)}\right), \end{aligned} \tag{6}$$

where

$$\frac{1}{\lambda_m(t_1,t_2)} \equiv \frac{1}{\lambda(t_1)} - \frac{1}{\lambda(t_2)}. \tag{7}$$

[3] The superscript "(t)" signifying the parameter to be that of the target shall be omitted from henceforth for convenience.

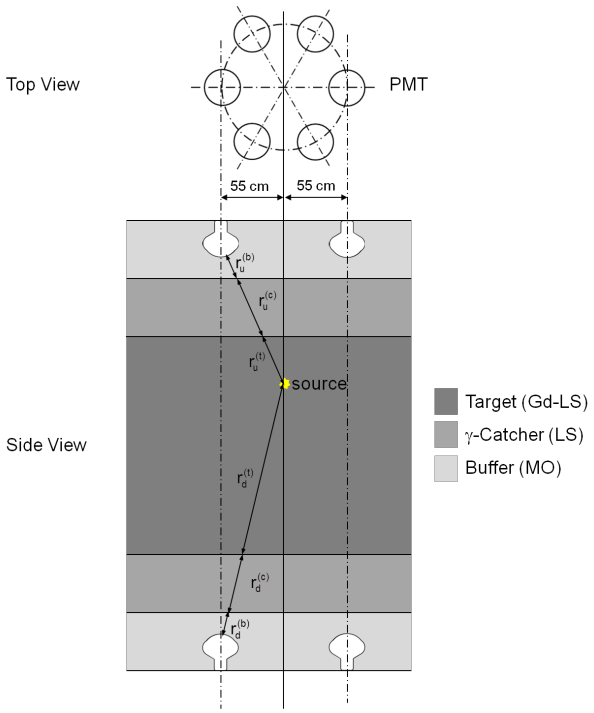

Figure 3: The location of six PMTs (solid line circle) nearest to the centerline of the detector at the top (u) and bottom (d) ends of the inner detector from above (not to drawn in scale). They are equally spaced at 55 cm from the centerline where calibration sources are deployed. The distance from any of the PMTs on either top or bottom and to the calibration source is the same. The path lengths between the radioactive source and the top (bottom) PMT in target, γ-catcher, and buffer are $r^{(t)}_{u(d)}$, $r^{(c)}_{u(d)}$, and $r^{(b)}_{u(d)}$, respectively.

Here $\Omega_{u(d)}$ is a geometrical factor and does not change over time. Thus the $\Omega_{u(d)}$ terms cancel out. If the angular efficiency profile of a PMT remains the same over time, then $\epsilon_{u(d)}(t_1)/\epsilon_{u(d)}(t_2)$ at any radioactive source position becomes constant at a given time. The term multiplied to the exponential of $-\Delta r_{ud}/\lambda_m(t_1, t_2)$, which contains the PMT performance model, is now marginalized to a constant coefficient with respect to the source position, i.e., with respect to Δr_{ud}. Therefore, if either $\lambda(t_1)$ or $\lambda(t_2)$ is known, the other can be calculated from the $\lambda_m(t_1, t_2)$, which can be obtained by plotting $R_{ud}(t_1)/R_{ud}(t_2)$ as a function of Δr_{ud} using Eq. 6.
To obtain $\lambda(t)$ at any given time t, $1/\lambda_m(t_1, t_2)$ is plotted as a function of Δr_{ud} with respect to a reference time $t_R = t_1$ against t_2. Here the time t is calculated to be the elapsed time in days since 2011-08-01. Here t_R is chosen to be 900 (901) days for far (near) detector, which is when the fifth (sixth) set of data samples is taken (See Table 2). Figure 4 shows $R(t_R)/R(t)$ as a function of Δr_{ud}, where t = 347 and 1 352 (346 and 1 351) days for far (near) detector. The resulting $1/\lambda_m(t_R, t)$ vs t for all data is shown in Fig. 5 and fit results with a second order polynomial is shown in Table 3. The point at t = 900 (901) days for the far (near) detector is not shown in Fig. 5 and not used in fitting $\lambda_m(t_R, t)$ with a second order polynomial since $\lambda_m(t_R, t = t_R) = 0$ by definition.

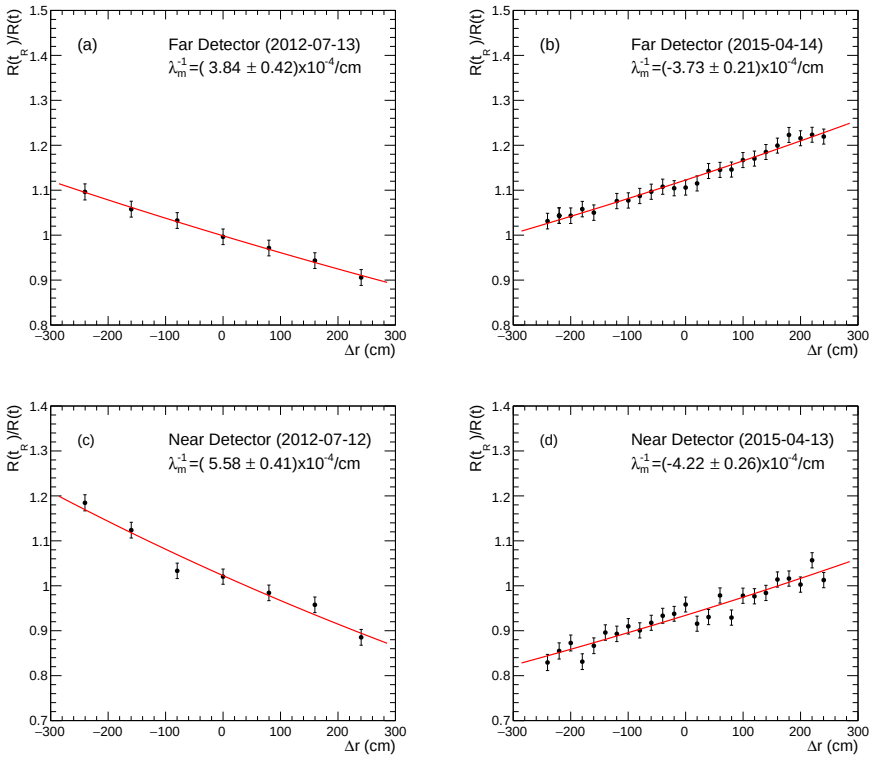

Figure 4: The ratio of ratios $R(t_R)/R(t)$ (see Eq. 6) for (a) far detector at 2012-07-13 (t = 347 days), (b) at 2015-04-12 (1351 days), (c) near detector at 2012-07-12 (346 days), and (d) at 2015-04-13 (1351 days) and t_R = 900 (901) days at 2014-01-17 (2014-01-18) since 2011-08-01 for far (near) detector, fit with an exponential function.

If the attenuation length is known at a given time, then the attenuation length between *in-situ* measurements can be calculated using Fig. 5. Assuming that the calculation of $1/\lambda_m(t_R, t)$ is valid at $t = t_R$, $\lambda(t_R)$ for a given $\lambda(t_0)$ can be obtained by $\lambda(t_R) = (1/\lambda_m(t_R, t_0) + 1/\lambda(t_0))^{-1}$, where $\lambda_m(t_R, t_0)$ is calculated from the fit results given in Table 3. Then using $\lambda_m(t_R, t)$ and $\lambda(t_R)$, $\lambda(t)$ at any given time within the region $\lambda_m(t_R, t)$ is valid can be obtained from $\lambda(t) = (1/\lambda(t_R) - 1/\lambda_m(t_R, t))^{-1}$.
For example, if the attenuation length of 12.0 ± 0.5 m at day 0 is assumed for both far and near detectors, the attenuation lengths of Gd-LS are calculated to have been degraded to 5.7 ± 0.3 m and 5.0 ± 0.3 m for

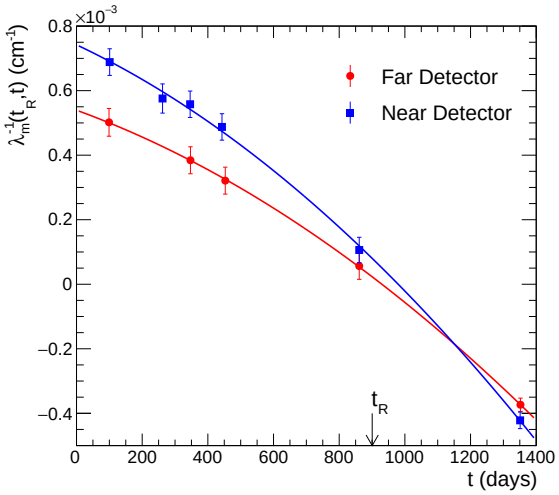

Figure 5: The relative inverse of attenuation lengths $1/\lambda_m(t_R, t)$ (see Eq. 7) as a function of the days since 2011-08-01 for far (red circles) and near (blue squares) detectors. The slope of $R(t_R)/R(t)$ represents the difference between the inverses of the attenuation length at a given time t in days and at the reference time t_R at 2014-01-17 (2014-01-18) for far (near) detector. The solid lines show the second order polynomial fits. The fit results are shown in Table 3.

Detector	p_0 ($\times 10^{-4}$ cm^{-1})	p_1 ($\times 10^{-7}$ cm^{-1}day^{-1})	p_2 ($\times 10^{-10}$ cm^{-1}day^{-1})
Far	5.39 ± 0.53	-3.71 ± 1.76	-2.25 ± 1.08
Near	7.42 ± 0.48	-4.70 ± 1.70	-2.90 ± 1.07

Table 3: Fit results of Fig. 5 with a second order polynomial $\lambda_m^{-1}(t_R, t) = p_0 + p_1\, t + p_2\, t^2$, where t is in days since 2011-08-01.

far and near detectors, respectively, over a period of about 1 350 days. The cause of this degradation of the attenuation length is under investigation.

5. Summary

A method is presented for measuring the relative attenuation length *in-situ* for the target Gd-LS at RENO experiment using radioactive sources without using a PMT performance model. It is found that the attenuation length of the Gd-LS in the RENO detectors has been degraded by about 50% over 1 350 days since the filling of the detectors assuming the initial attenuation length of Gd-LS at beginning of the experiment is greater than ~ 10 m.

Acknowledgments

The RENO experiment is supported by the National Research Foundation of Korea (NRF) grant No. 2009-0083526 funded by the Korea Ministry of Science, ICT & Future Planning. Some of us have been supported by a fund from the BK21 of NRF. We gratefully acknowledge the cooperation of the Hanbit Nuclear Power Site and the Korea Hydro & Nuclear Power Co., Ltd. (KHNP).

[1] M. Apollonio *et al.* [CHOOZ Collaboration], Phys. Lett. B **420**, 397 (1998)

[2] M. Apollonio *et al.* [CHOOZ Collaboration], Eur. Phys. J. C **27**, 331 (2003)

[3] S. H. Seo *et al.* [RENO Collaboration], to be submitted to Phys. Rev. D.

[4] J. S. Park *et al.*, Nucl. Instrum. Meth. A **707**, 45 (2013).

[5] L. Gao *et al.*, Chin. Phys. C **37**, 076001 (2013).

[6] J. K. Ahn *et al.* [RENO Collaboration], arXiv:1003.1391 [hep-ex].

[7] I. S. Yeo *et al.*, Phys. Scripta **82**, 065706 (2010).

[8] K. S. Park *et al.*, Nucl. Instrum. Meth. A **686**, 91 (2012).

[9] H. S. Kim, New Physics: Sae Mulli 62, 631 (2012).